



Research papers

Recent dynamics of alpine lakes on the endorheic Changtang Plateau from multi-mission satellite data



Kehan Yang^{a,b,c}, Fangfang Yao^d, Jida Wang^d, Jiancheng Luo^{a,b,*}, Zhanfeng Shen^{a,b}, Chao Wang^e, Chunqiao Song^f

^a Institute of Remote Sensing and Digital Earth, Chinese Academy of Sciences, Beijing, China

^b University of Chinese Academy of Sciences, Beijing, China

^c Department of Geography, Institute of Arctic and Alpine Research, University of Colorado at Boulder, Boulder, CO, USA

^d Department of Geography, Kansas State University, Manhattan, KS, USA

^e Department of Environmental Sciences, University of Puerto Rico, Rio Piedras, San Juan, PR, USA

^f Department of Geography, University of California, Los Angeles, CA, USA

ARTICLE INFO

Article history:

Received 6 February 2017

Received in revised form 8 June 2017

Accepted 12 July 2017

Available online 14 July 2017

This manuscript was handled by K. Georgakakos, Editor-in-Chief, with the assistance of Venkat Lakshmi, Associate Editor

Keywords:

Alpine lakes

Changtang Plateau

Inter- and Intra-annual variations

Climate change

Landsat

Huanjing satellites

ABSTRACT

Monitoring of the alpine lakes on the endorheic Changtang Plateau is vitally important in understanding climate impacts on hydrological cycle. Existing studies have revealed an accelerated lake expansion on the Changtang Plateau during the 2000s compared with prior decades. However, the partial hiatus of recent Landsat archive affected the continuation of understanding the lake changes in the recent decade. Here we synergistically used imagery from Landsat and Huanjing satellites to enable a detailed monitoring of lake area dynamics on the Changtang Plateau. Our results present that lakes on the Changtang Plateau continued to expand at a rapid rate of $340.79 \text{ km}^2 \text{ yr}^{-1}$ ($1.06\% \text{ yr}^{-1}$, $p < 0.05$) from 2009 to 2014. Changes in endorheic (terminal) lakes contribute to 98% of the net expansion, suggesting that monitoring endorheic lake dynamics is of critical importance for understanding climate changes. Meanwhile, changes in saline lakes, which are mostly endorheic, account for 96% of the net expansion, implying that the proportion of freshwater storage on the Changtang Plateau is likely in decline. Rapid expansion occurred in both glacier-fed and non-glacier-fed lakes, with a rate of $224.94 \text{ km}^2 \text{ yr}^{-1}$ ($0.92\% \text{ yr}^{-1}$, $p < 0.05$) and $115.85 \text{ km}^2 \text{ yr}^{-1}$ ($1.47\% \text{ yr}^{-1}$, $p = 0.08$), respectively, indicating that glacier retreat alone may not fully explain the recent lake expansion. Intra-annual variations of the selected 24 large lakes fluctuated within 0.22–2.46% (in coefficient of variation) for glacier-fed lakes and 0.17–2.36% for non-glacier-fed lakes. Most of these lakes expanded during the unfrozen period (from May/June to October) and reached to their maximum extents in September or October. By spatially associating our revealed lake changes with climate variables, we observed that the recent lake expansion is more related to precipitation than to temperature, although future efforts are needed for a more comprehensive picture of the lake changing mechanisms.

© 2017 The Authors. Published by Elsevier B.V. This is an open access article under the CC BY-NC-ND license (<http://creativecommons.org/licenses/by-nc-nd/4.0/>).

1. Introduction

Alpine lakes are crucial hydrologic components and extremely sensitive to climate change in arid and semi-arid endorheic watersheds (Williamson et al., 2009). One of the world's largest alpine lake groups is found on the endorheic basins of Changtang Plateau (CP) in the northwestern Tibetan Plateau (TP) (Fig. 1) (Rizvi, 1999), where the average elevation exceeds 4000 m a.s.l (Qiu, 2008). Due to minimal human activities, the water balance of these endorheic

basins is dominantly controlled by regional climate (Haas et al., 2011; Sheng and Yao, 2009). During the past 50 years, the CP has undergone a much faster warming trend ($\sim 0.447^\circ\text{C}$ per decade) than the global average ($0.15\text{--}0.20^\circ\text{C}$ per decade) (Hansen et al., 2010; Xu et al., 2008). This sustained warming trend has resulted in significant glaciers retreat and permafrost thawing, thus contributing to feeding alpine lakes (Ersi et al., 2010; Lei et al., 2012; Yang et al., 2010). In addition to meltwater from glaciers and permafrost, precipitation also plays an important role in supplying water to these lakes, especially in the context of the general increase in precipitation over recent decades (Rangwala et al., 2009). Therefore, to uncover the impacts of the accelerated climate change on alpine lakes of the CP, it is vitally important to continue

* Corresponding author at: Institute of Remote Sensing and Digital Earth, Chinese Academy of Sciences, 20A Datun Road, Chaoyang District, Beijing 100101, China.

E-mail address: Luojc@radi.ac.cn (J. Luo).

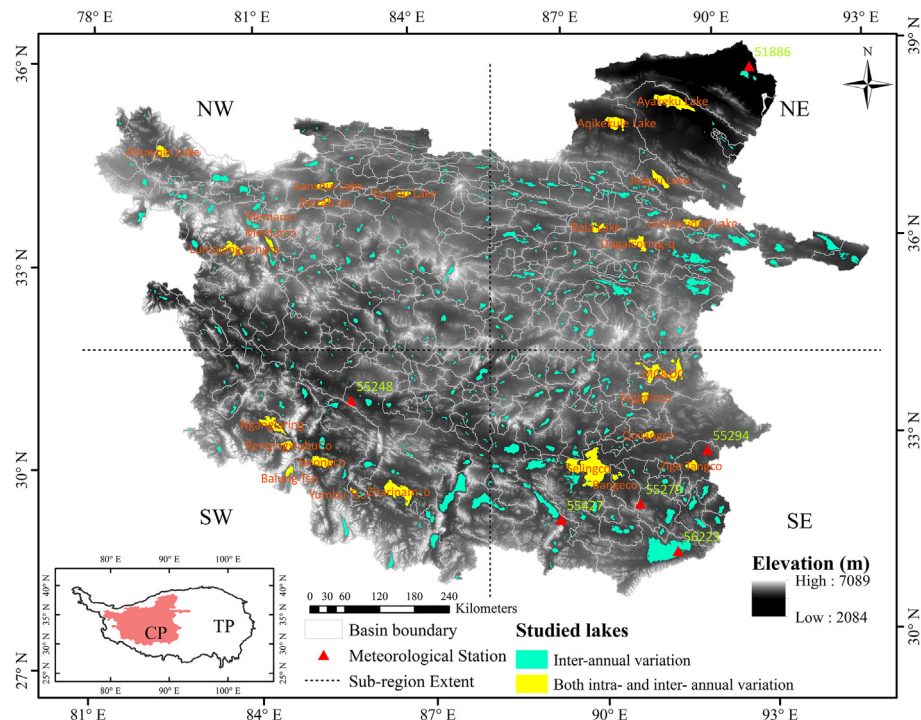


Fig. 1. The Changtang Plateau (CP) and studied lakes (874 in total). Boundaries of the CP and TP were determined from the 15-s HydroSHEDS drainage basin dataset (Lehner et al., 2006). Numbers 55248, 51886, 56223, 55427, 55294 and 55279 are codes of available meteorological stations on the CP. NW, NE, SW and SE stand for northwest, northeast, southwest and southeast sub-regions of the CP, respectively.

monitoring the dynamics of these alpine lakes to comprehensively understand the mechanisms of climate change forcing on the regional hydrological cycles on the CP (Song et al., 2014a; Zhang et al., 2011a).

Due to the harsh environment on the CP and few in situ observation stations, satellite remote sensing has become an indispensable tool for studying the dynamics of the alpine lakes (Huang et al., 2011; Lei et al., 2014; Li and Sheng, 2013; Li et al., 2014; Liao et al., 2013; Song et al., 2016, 2017; Wan et al., 2016; Zhang et al., 2014b). The advent of satellite datasets makes it possible for long-term and large-scale monitoring of alpine lakes. For example, by extracting lakes from Landsat imagery, Li and Sheng (2013) studied the spatiotemporal dynamics of the CP lakes from 1976 to 2009, and revealed an accelerated lake expansion trend in the 2000s compared with that of previous decades (1970–1990s). Recently, much attention has been paid to understanding the expansion of Tibetan lakes during the latest decade (Pekel et al., 2016; Song et al., 2014b; Wan et al., 2016; Zhang et al., 2017a,b). However, temporal resolutions of these investigations are mostly limited to multi-year to decadal levels, which are insufficient for a complete picture of recent alpine lake dynamics. In addition, the intra-annual pattern of the alpine lakes, driven by strong seasonal climate variations (Indian monsoon in summer and westerlies in winter), is rarely studied in previous studies.

Despite the importance, monitoring alpine lake dynamics on the CP at both high spatial and temporal resolutions has been challenging, particularly given the partial hiatus of recent Landsat archive due to the scan line corrector (SLC) failure in Landsat 7 since May 2003, the poor coverage of Landsat 5 on the CP after 2009, and the unavailability of Landsat 8 until May 2013 (Arvidson et al., 2002; Ju and Roy, 2008). Fortunately, Huanjing 1A and 1B (HJ-1A/1B), China's environmental twin satellites, were launched in September 2008, which have ever since provided continuous observations of the Earth at a 30-m resolution with a 2-day revisit period. The sensor aboard each HJ satellite records surface

reflectance in 4 spectral bands (blue, green, red and near infrared (NIR)) with a wide swath width of 700 km, making its imagery highly suitable for monitoring spatiotemporal variations of water bodies over large areas. Therefore, combining imagery archived from both Landsat and HJ satellites will provide high spatiotemporal monitoring of alpine lakes across the entire CP.

Our study aims to improve the understanding of recent dynamics of the alpine lakes across the entire CP through a comprehensive monitoring of the lake extents from 2009 to 2014. By combining the HJ-1A/1B and Landsat imagery synergistically, we developed a systematic lake mapping framework to: 1) map all 874 lakes bigger than 1 km² at a yearly temporal resolution to characterize their inter-annual variations, and 2) map 24 selected lakes bigger than 50 km² at a monthly resolution during the unfrozen period to characterize both of their inter- and intra-annual variations. This mapping, to our best knowledge, achieves some of the finest temporal resolution among alpine lake studies for the entire CP and thus improves our understanding of alpine lake dynamics in seasonal scale. Our monitoring period also completely includes the recent hiatus in Landsat imagery. Following the introduction, Section 2 describes the studied lake regions and the used materials, while the detailed methodology is explained in Section 3. Section 4 presents our mapping consistency and lake area dynamics. Section 5 discusses the possible lake changing mechanism by analyzing the relationship between lake area and climate factors for each endorheic basin. Conclusions and further implications are summarized in Section 6.

2. Study area and datasets

2.1. Study area

Covering a total area of ~709,218 km² (accounting for ~28% of the entire TP), the CP (Fig. 1) consists of 400 endorheic drainage basins with an average elevation of 4,894 m a.s.l.. It is home to

66% of the TP lakes in area and 55% in number, with an average lake density of $\sim 0.026 \text{ km}^{-2}$ (Zhang et al., 2014b). In particular, the remote environmental settings and thus minimal human activities make the CP an ideal region for studying lake dynamics in response to climate change.

The climate across the CP ranges from temperate arid to sub-arctic semi-humid (Song et al., 2013). Dominated by the Indian monsoon in summer and cold and dry westerlies in winter, the climate indicates a strong seasonal variation (Yao et al., 2012). At least 60–90% of the total annual precipitation falls between June and September, while less than 10% falls in winter between November and February (Xu et al., 2008). The average annual temperature on the CP is generally near or below 0°C (Sheng and Yao, 2009). Lakes on the southern CP region are generally unfrozen between May and October, while those on the northern CP region are unfrozen between June and October.

All lakes bigger than 1 km^2 on the CP were studied at a yearly resolution between 2009 and 2014. 24 lakes bigger than 50 km^2 were selected to monitor their monthly changes during the unfrozen period. These lakes were sampled across the entire CP, and cover all studied water types, including saline and freshwater lakes, glacier-fed and non-glacier-fed lakes, endorheic and exorheic lakes (see Fig. 1 and Table 1).

2.2. Optical satellite images

Landsat imagery is one of the most broadly used satellite datasets for lake mapping (Feyisa et al., 2014). However, the available number of high quality imagery is reduced because the CP is poorly covered by Landsat 5 after 2009 and the new Landsat 8 was not available until April 2013. Huanjing (HJ) satellites serve as an alternative data source, which were launched on September 6, 2008 and have been used for mapping water extent effectively since then (Liao et al., 2014; Lu et al., 2011). As shown in Table 2, HJ imagery (HJ-1A/1B) has the same spatial resolution (30 m) as Landsat imagery but a much higher temporal resolution (2 days); it has 4 spectral bands (blue, green, red and NIR) which are similar to those of Landsat imagery and has a wider swath width (700 km). These

properties make HJ imagery highly suitable for monitoring surface water changes over large geographic areas. In this study, we used the imagery acquired by Landsat-5 TM, Landsat-7 ETM+, Landsat-8 OLI, HJ-1A CCD, and HJ-1B CCD to study the spatiotemporal patterns of the CP lakes. The combination of multi-mission satellite data substantially improves the temporal resolution of lake mapping. Landsat and HJ satellites images were downloaded from the USGS Earth Resources Observation and Science Center (<https://eros.usgs.gov>) and the China Center for Resources Satellite Data and Application (<http://www.cresda.com>), respectively.

2.3. Drainage watershed boundaries and sinks

We used the 15 arc-second HydroSHEDS dataset (Lehner et al., 2006) (<http://hydrosheds.cr.usgs.gov>) to extract endorheic catchments and their drainage termini (i.e., sinks) across the CP. HydroSHEDS include several hydrographic data layers such as drainage basins, drainage directions, and river networks, which were derived from the digital elevation model (DEM) acquired by the Shuttle Radar Topography Mission (SRTM) in February 2000. The applied SRTM DEM went through a sequence of surface corrections such as void filling and filtering, in order to remove spurious sinks and derive more accurate hydrologic topology. In our case, the drainage basin layer was used to extract a total of 400 endorheic catchments on the CP, and the drainage direction layer was applied to identify the sink location in each endorheic basin. These identified sink points were then overlaid upon our studied lakes to determine whether a lake is endorheic (i.e., spatially concurrent with a sink) or exorheic.

2.4. Freshwater and saline lakes

The distinction between fresh and saline water for each studied CP lake was referred to the documented salinity in the Chinese Lake Catalogue (Wang and Dou, 1998). For any undocumented lake, we used the same method as in Wang et al. (2015, 2016) to determine its water type. In brief, a lake is considered to be saline if (1) its location concurs with the sink of an endorheic basin,

Table 1
Selected 24 large lakes and their limnologic properties.

Lake name	Coordinate (lon/lat)	Area (km^2)	Elevation (m a.s.l.)	Saline	Glacier-fed	Endorheic	Sub-region
Aksayqin Lake	79.87, 35.21	238.85	4844	Yes	Yes	Yes	NW
Lumajangdongco	81.61, 34.02	377.68	4812	Yes	Yes	Yes	NW
Jianshui Lake	83.10, 35.29	187.63	4889	Yes	Yes	Yes	NW
Memarco	82.31, 34.22	161.27	4920	Yes	Yes	Yes	NW
Yanghu Lake	84.61, 35.42	154.89	4779	Yes	Yes	Yes	NW
Bairab co	83.13, 35.04	136.84	4960	Yes	No	Yes	NW
Ayakeku Lake	89.43, 37.54	949.80	3876	Yes	Yes	Yes	NE
Dogaicoring-q	89.24, 35.32	377.24	4787	Yes	Yes	Yes	NE
Jingyu Lake	89.44, 36.33	328.76	4713	Yes	Yes	Yes	NE
Lexiewudan Lake	90.19, 35.75	268.15	4870	Yes	Yes	Yes	NE
Aqikekule Lake	88.41, 37.08	507.23	4251	Yes	Yes	Yes	NE
Rola Lake	88.38, 35.41	208.07	4828	Yes	Yes	Yes	NE
Silingco	89.02, 31.80	2375.62	4546	Yes	Yes	Yes	SE
MC&DC	90.07, 33.44	1038.45	4935	Yes	Yes	Yes	SE
Zige Tangco	90.86, 32.08	238.07	4568	Yes	No	Yes	SE
Qixiangco	89.98, 32.45	185.09	4615	Yes	No	Yes	SE
Yaggainco	89.80, 33.02	147.74	4872	Yes	No	Yes	SE
Bangeco	89.51, 31.75	126.59	4527	Yes	No	Yes	SE
Zharinamco	85.61, 30.93	1005.58	4612	Yes	Yes	Yes	SW
Tarongco	84.12, 31.14	487.93	4567	No	Yes	No	SW
Nganglaring	83.08, 31.54	503.01	4716	Yes	Yes	Yes	SW
Balung Tso	83.58, 30.89	146.26	5101	Yes	Yes	Yes	SW
Renqingxiubuco	83.45, 31.28	188.67	4760	Yes	Yes	Yes	SW
Yumbu Tso	84.79, 30.80	64.78	4640	Yes	No	Yes	SW

Note: MC&DC stands for Dorsoidongco and Migrigyangzhamco lakes. We consider these two lakes as one entity as they have merged into one lake as a result of recent expansion. Accordingly, their catchments are also considered as one basin in the sections below. Please refer to Fig. 1 for sub-region locations.

Table 2

Parameters of HJ-1A/1B CCD imagery compared to those of Landsat imagery used in this study.

Sensor	HJ-1A/1B CCD	Landsat-5 TM	Landsat-7 ETM+	Landsat-8 OLI
Band blue (μm)	0.43–0.52	0.45–0.52	0.45–0.52	0.45–0.52
Band green (μm)	0.52–0.60	0.52–0.60	0.52–0.60	0.52–0.60
Band red (μm)	0.63–0.69	0.63–0.69	0.63–0.69	0.63–0.68
Band near-infrared (μm)	0.76–0.90	0.76–0.90	0.75–0.90	0.85–0.89
Spatial resolution (m)	30	30	30	30
Revisit time (day)	2	16	16	16
Swath width (km)	700	185	185	185

where dissolved salt likely accumulates as no surface outflow is allowed, or (2) its surface and lateral regions indicate evident spectral trails of saturated salt or evaporite deposition. As described in Section 2.3, sink points were identified from the 15 arc-second HydroSHEDS drainage direction data (Lehner et al., 2006), and spectral evidence of salt was inspected with the assistance of high-resolution Google Earth imagery. Other available literature was used to ensure the overall accuracy of assigned water types.

2.5. Glacier and permafrost dataset

The Second Glacier Inventory of China (Guo et al., 2014) (<http://westdc.westgis.ac.cn>) was used to calculate the glacier coverage in each basin on the CP and to examine whether each lake was supplied by glacial meltwater (Phan et al., 2013). Permafrost coverage in each basin was calculated based on the 1:3,000,000 Map of Permafrost Distribution on the Tibetan Plateau produced by Li and Cheng. (1996) (<http://westdc.westgis.ac.cn>).

2.6. Temperature and precipitation dataset

Due to extremely few meteorological stations located on the CP, the Moderate Resolution Imaging Spectroradiometer (MODIS) Land Surface Temperature (LST) daily product MOD11A (<http://reverb.echo.nasa.gov>) and the Tropical Rainfall Measuring Mission (TRMM) monthly product 3B43 (Huffman et al., 2007) (<https://pmm.nasa.gov/data-access/downloads/trmm>) were used to estimate the trend of temperature and precipitation, respectively. We only used the night time temperature of MOD11A because it is much more accurate than the day time temperature on the Tibetan region (Schneider et al., 2009; Zhang et al., 2014a). In situ daily observation data of all 6 meteorological stations available on the CP were used to validate the accuracy of MODIS LST and TRMM precipitation products.

3. Methods

3.1. Image preprocessing

108 HJ images and 19 Landsat images were used to map yearly water extents of all studied lakes bigger than 1 km² from 2009 to 2014. Most lakes (96%) were extracted from images in September or October when lake areas are relatively stable (Lei et al., 2013; Song et al., 2014b), while the rest (4%) were extracted from images in late August or November because no cloud-free images are available in September or October. 318 HJ images and 246 Landsat images (including 88 ETM + images) were used to map monthly water extents of the 24 selected lakes bigger than 50 km² during the unfrozen period (from May or June to October) from 2009 to 2014. An SCL-off ETM + image was only considered when its reflectance gaps could be compensated by another image acquired in an adjacent month. All images were georeferenced with a root mean square error (RMSE) lower than 30 m. Top-of-atmosphere (TOA)

reflectance of all imagery was calculated from the digital numbers using the corresponding calibration parameters.

3.2. Lake extent mapping

The band index method has been widely used for water mapping from remote sensing images (Jiang et al., 2014). Among different water indices, only Normalized Difference Water Index (NDWI) (McFeeters, 1996) (Eq. (1)) and High Resolution Water Index (HRWI) (Yao et al., 2015) (Eq. (2)) can be calculated from both Landsat and HJ imagery. We chose HRWI in this study because HRWI appears to be more robust in detecting lake extent under various water conditions than NDWI (Yao et al., 2015).

$$\text{NDWI} = (G - \text{NIR}) / (G + \text{NIR}) \quad (1)$$

$$\text{HRWI} = 6 \times G - R - 6.5 \times \text{NIR} + 0.2 \quad (2)$$

where G, R, NIR are the reflectance in green, red, and near-infrared bands, respectively.

In order to accurately detect water boundary for each lake, we implemented a systematic lake mapping framework (Fig. 2) which consists of two main procedures: automated mapping (AM) and quality assurance (QA). In the AM process, the HRWI images were calculated to enhance the spectral contrast between land and water, and then candidate lake extents were flagged by segmenting the HRWI images using a global threshold T (here, T = 0). For each identified water body, an adaptive histogram segmentation algorithm based on the spectral contrast between the water body and its local background was applied to fine-tune its boundary (see Li and Sheng. (2012), Lyons et al. (2013) and Qiao et al. (2012) for details). Although the automatic lake mapping scheme is highly reliable, it is necessary to apply post-processing to achieve lake mapping result at its best quality (Li and Sheng, 2012; Sheng et al., 2016; Wang et al., 2014). In the QA process, we performed a rigorous visual interpretation to eliminate any remaining mapping errors with the assistance of a Graphical User Interface (GUI) mapping tool (Wang et al., 2014).

3.3. Analysis of changing trends and variations in lake area

The changing trends in lake areas, computed using the best-fit linear regression, were applied to quantify the inter-annual variations in lake areas. It is worth noting that some individual lakes have merged into one water body as a consequence of lake area expansion over time. If this event happens, those separated lakes were considered as one lake in the change analysis. To assess the intra-annual variations of 24 large lakes, each lake was firstly evaluated by the monthly annual cycle averaged within the studied 6 years. The variations of the averaged lake areas were then quantified by the coefficient of variation (c_v):

$$c_v = \frac{\sigma}{\mu} \quad (3)$$

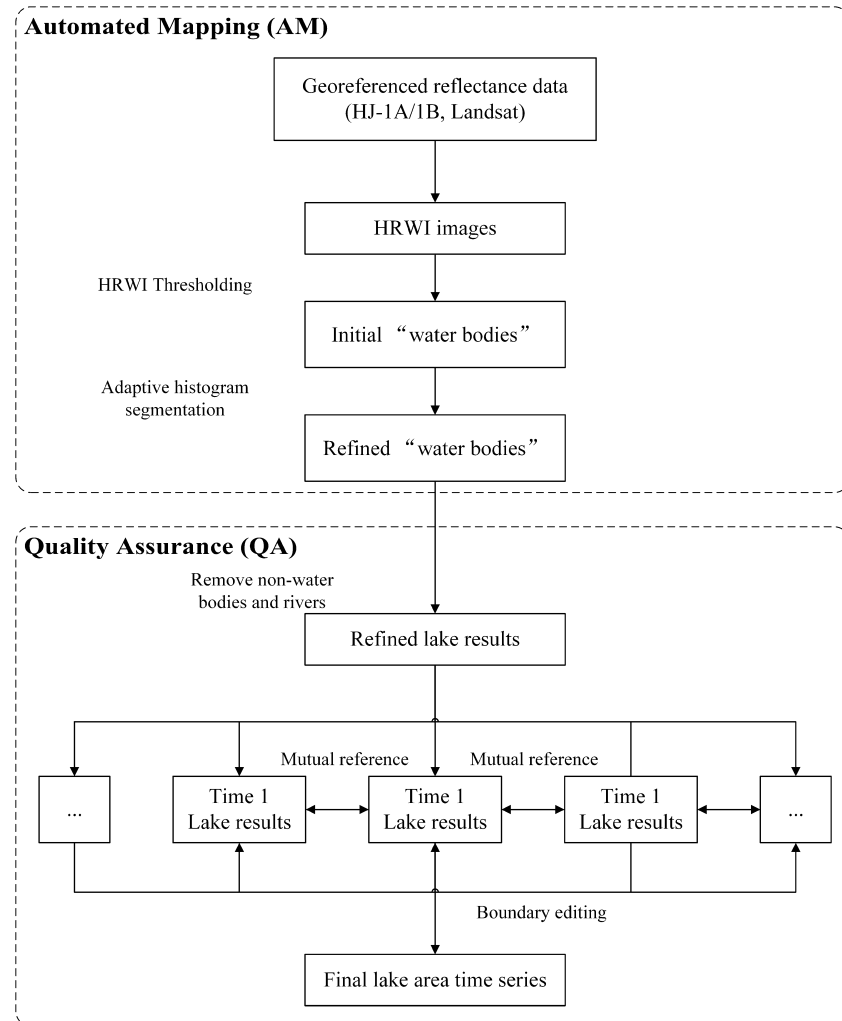


Fig. 2. Flowchart of applied lake mapping framework.

where σ and μ are the standard deviation and mean of lake areas, respectively. Compared to standard deviation, the coefficient of variation is a unitless metric to measure the scale of variability relative to the mean, and thus more appropriate to compare intra-annual variations for lakes that are in different sizes. In this study, the intra-annual variations were only quantified during lake unfrozen months every year, because the ice and snow cover during lake frozen months blur the lake boundaries in imagery and the lake extents thus cannot be accurately detected by the proposed methodology.

4. Results

4.1. Consistency of lake mapping using Landsat and HJ images

In order to assess the consistency of lake extents mapped from Landsat and HJ satellites, a total of 376 pairs of lake extents mapped from Landsat and HJ satellites images were compared. For each compared pair, the acquisition dates of the two images are closer than 2 days, in order to minimize uncertainties due to short-term lake boundary variations. As shown in Fig. 3, lake areas extracted from HJ imagery agree well with those from Landsat imagery (Slope ≈ 1.00 , $R^2 > 0.99$), indicating that lake extents mapped from Landsat and HJ satellites are highly consistent and

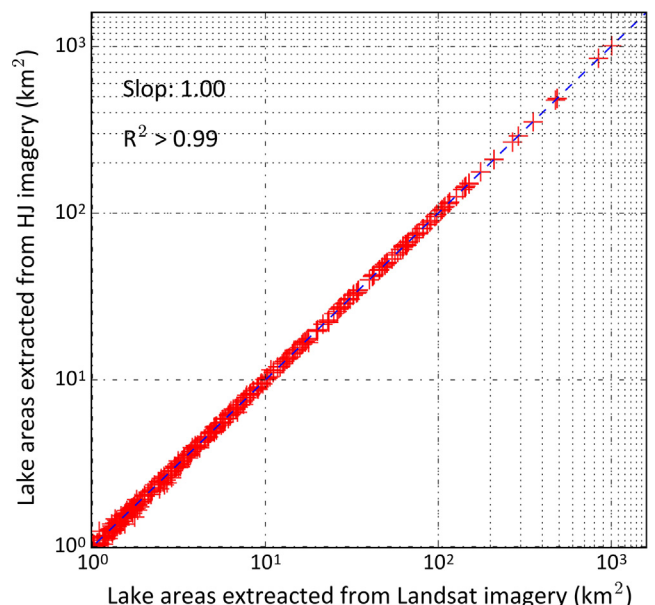


Fig. 3. Comparison between lake mappings from Landsat and HJ satellite images.

a mixed usage of these images will not affect the validity of our calculated lake changes.

4.2. Inter-annual variations for all studied lakes

As illustrated in Fig. 4, the majority of the CP lakes continued to expand from 2009 to 2014, but the changing rate exhibited a strong spatial heterogeneity across the CP. In general, the expansion rate follows a south-to-north increasing gradient. For example, most lakes in Region NE expanded faster than 1.00 yr^{-1} while lakes in the Region SW were generally stable or shrinking. Lakes within Region NW and Region SE, however, indicate evident opposite changing patterns. For example, most lakes in the blue-outlined basins rapidly expanded, whereas lakes in the red basins generally shrank (see Fig. 4).

Inter-annual variations of water area for different types of lakes are summarized in Fig. 5 and Table 3. The total lake area on the CP expanded from $31,004.15\text{ km}^2$ in 2009 to $32,732.59\text{ km}^2$ in 2014, with a significant net changing trend of $340.79\text{ km}^2\text{ yr}^{-1}$ ($1.06\%\text{ yr}^{-1}$, $p < 0.05$). 558 lakes expanded with an overall rate of $422.66\text{ km}^2\text{ yr}^{-1}$ ($1.55\%\text{ yr}^{-1}$, $p < 0.05$) while the other 316 lakes shrank with an overall rate of $-81.87\text{ km}^2\text{ yr}^{-1}$ ($-1.63\%\text{ yr}^{-1}$).

Endorheic lakes occupy 84% of the total lake area on the CP (see Fig. 6). These lakes show a significant expanding rate of $334.61\text{ km}^2\text{ yr}^{-1}$ ($1.24\%\text{ yr}^{-1}$, $p < 0.05$), explaining 98% of the net increase from all studied lakes, while the exorheic lakes indicate a much slower expansion ($6.18\text{ km}^2\text{ yr}^{-1}$ or $0.12\%\text{ yr}^{-1}$), accounting for only 2% of the net increase. This implies that endorheic lakes are more sensitive to the variations in water inflow, and monitoring their changes is of critical importance for understanding regional climate change.

Saline lakes have an average area of $28,974.31\text{ km}^2$, accounting for 90% of the total lake area. These lakes, which are most endorheic (see Fig. 6), expanded at a rate of $326.80\text{ km}^2\text{ yr}^{-1}$ ($1.13\%\text{ yr}^{-1}$). However, freshwater lakes were stable with a minor change

of $13.99\text{ km}^2\text{ yr}^{-1}$ ($0.43\%\text{ yr}^{-1}$). Therefore, the proportion of fresh-water resources storage on the CP is likely in decline.

Lakes without glacier supply (720 lakes) largely outnumber those fed by glaciers (154 lakes) (see Fig. 6), but glacier-fed lakes occupy a much larger area ($24,336.38\text{ km}^2$, in comparison with $7,899.732\text{ km}^2$ for non-glacier-fed lakes). Glacier-fed lakes exhibited a significant expansion of $224.94\text{ km}^2\text{ yr}^{-1}$ ($0.92\%\text{ yr}^{-1}$, $p < 0.05$), accounting for 66% of the net area increase in all lakes. Non-glacier-fed lakes also expanded at a rapid rate of $115.85\text{ km}^2\text{ yr}^{-1}$ ($1.47\%\text{ yr}^{-1}$), accounting for the other 34% of the net area increase. As we show in Table 3, although glacier-fed lakes are dominant in area, the number of expanding glacier-fed lakes (115 lakes) is much less than that of non-glacier-fed expanding lakes (443 lakes). Moreover, the widely distributed non-glacier-fed lakes have an even greater overall expanding rate ($1.47\%\text{ yr}^{-1}$) compared with that of glacier-fed lakes ($0.92\%\text{ yr}^{-1}$). These indicate that glacier melting cannot fully explain the observed lake expansion on the CP.

4.3. Inter-annual and intra-annual variations for large lakes

Fig. 7a–d (the left panel) show monthly variations of the 24 large lakes in the unfrozen months from 2009 to 2014. Six studied lakes in the Region NE (Fig. 7b) expanded with similar patterns of variations while those in the Region SW (Fig. 7d) have nearly the same stable pattern. Most lakes in Regions NW and SE (Fig. 7a and c) expanded but some lakes (such as Jianshui Lake and Yaggainco) have more rapid expansion.

The detailed intra-annual variations for each large lake were further evaluated by the monthly annual cycle averaged within the studied 6 years (right panel in Fig. 7). Most lakes expanded from May or June to October, reaching to the maximum extents in September or October. In Region NW, the five glacier-fed lakes expanded with different patterns. Aksayqin Lake, Jianshui Lake and Yanghu Lake expanded with similar patterns, with coefficient

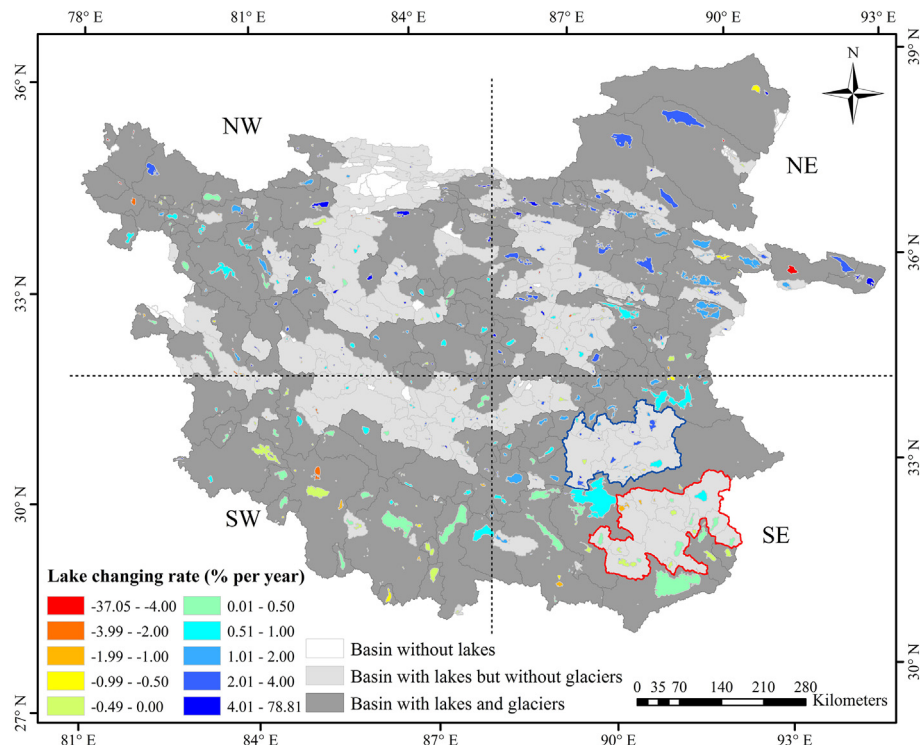


Fig. 4. Inter-annual trends of all studied alpine lakes ($>1\text{ km}^2$) on the CP from 2009 to 2014. The blue and red outlines in the SE illustrate two typical regions with opposite lake changing patterns. (For interpretation of the references to colour in this figure legend, the reader is referred to the web version of this article.)

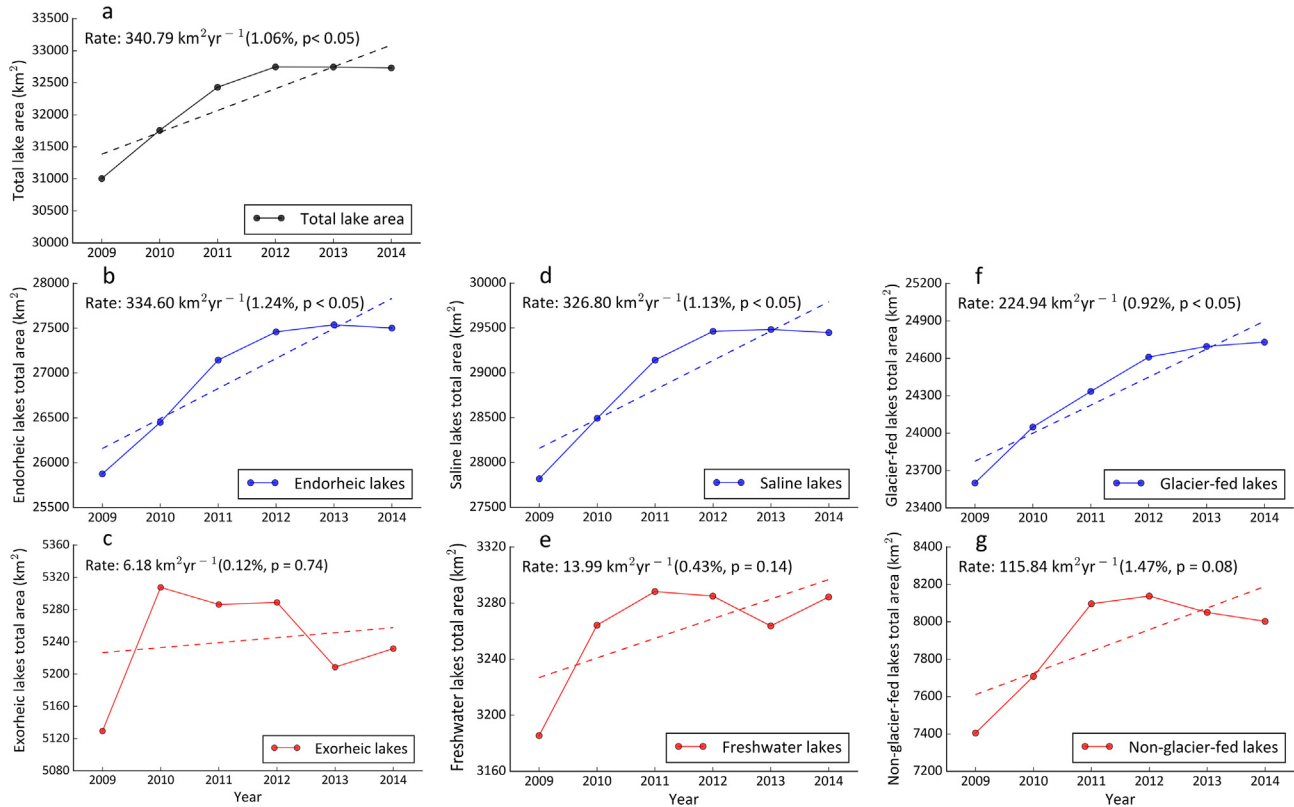


Fig. 5. Inter-annual variations of different types of lakes on the CP during 2009–2014. (a–g) Inter-annual area variations for all lakes, endorheic lakes, exorheic lakes, saline lakes, freshwater lakes, glacier-fed lakes and non-glacier-fed lakes, respectively.

Table 3

Statistics of inter-annual variations of alpine lakes ($>1 \text{ km}^2$) on the CP.

Category	Net change (yr^{-1})			Change in expanding lakes (yr^{-1})			Change in significant expansion lakes (yr^{-1})			Change rate of shrinkage lakes (yr^{-1})			Change rate of significant shrinkage lakes (yr^{-1})		
	Area (km^2)	% of mean	Lake number	Area (km^2)	% of mean	Lake number	Area (km^2)	% of mean	Lake number	Area (km^2)	% of mean	Lake number	Area (km^2)	% of mean	Lake number
All lakes	340.79	1.06*	874	422.66	1.55*	558	330.32	1.83*	210	-81.87	-1.63*	316	-38.71	-7.15*	30
Endorheic	334.61	1.24*	326	362.98	1.49*	255	309.89	1.76*	139	-28.38	-1.05	71	-8.86	-4.09*	8
Exorheic	6.18	0.12	548	59.67	2.03*	303	20.42	3.96*	71	-53.49	-2.33*	245	-29.95	-9.16*	22
Freshwater	13.99	0.43	351	53.46	2.94*	213	26.61	6.37*	63	-39.47	-2.74*	138	-26.75	-12.74*	10
Saline	326.80	1.13*	523	369.20	1.45*	345	303.71	1.72*	147	-42.40	-1.19	178	-11.96	-3.61*	20
Glacier-fed	224.94	0.92*	154	270.56	1.26*	115	243.62	1.60*	58	-45.62	-1.61*	39	-31.74	-7.49*	6
Non-glacier-fed	115.85	1.47	720	152.09	2.65*	443	86.70	3.07*	152	-36.25	-1.67	277	-6.97	-5.91*	24

Note: "Significant expanding (or shrinking) lakes" refer to the individual lakes that all exhibit increasing (or decreasing) trends with p-values less than 0.05. *** indicates that the inter-annual trend in the aggregated lake area is significant.

of variation (c_v) ranging from 1.32% to 2.46%, while the area of Lumajangdongco remained stable during the lake unfrozen period. The lake area of non-glacier-fed Bairab co increased from June to August and decreased from August to October, which does not resemble any of the other five glacier-fed lakes. In Region NE, lakes significantly expanded from June to September and became relatively stable during September to October. The patterns of intra-annual variations in those lakes are similar, with coefficient of variation (c_v) ranging from 0.73% to 1.53%. In Region SE, the two glacial-fed lakes (Silingco and MC&DC) expanded in similar patterns while the expansion patterns of the other four non-glacial-fed lakes are quite different. For example, Zige Tangco has the maximum lake extent in July while Bangeco shrank from May to June and then expanded until October. The four non-glacial-fed lakes have higher intra-annual variations (c_v ranging from 0.53% to 2.36%) compared with those of the two glacier-fed lakes (c_v ranging from 0.45% to 0.49%). In Region SW,

the non-glacier-fed lake (Yumbu Tso) and the other five glacial-fed lakes have nearly the same stable pattern (c_v ranging from 0.17% to 0.43%) and show slightly expanding trends. For the entire CP, intra-annual variations in lake extent fluctuate with 0.22–2.46% for glacier-fed lakes and 0.17–2.36% for non-glacier-fed lakes.

5. Discussion

We contributed to improving the understanding of lake changing patterns on the CP in recent years by monitoring all lakes bigger than 1 km^2 at a yearly resolution and 24 selected lakes bigger than 50 km^2 at a monthly resolution during unfrozen period. This mapping, to our knowledge, achieves some of the finest temporal resolution among alpine lake studies for the entire CP. Our results show that alpine lakes on the CP continued to expand from 2009 to 2014, which agrees well with the lake level dynamics study of Jiang et al. (2017) for a similar period. However, the mechanism of the

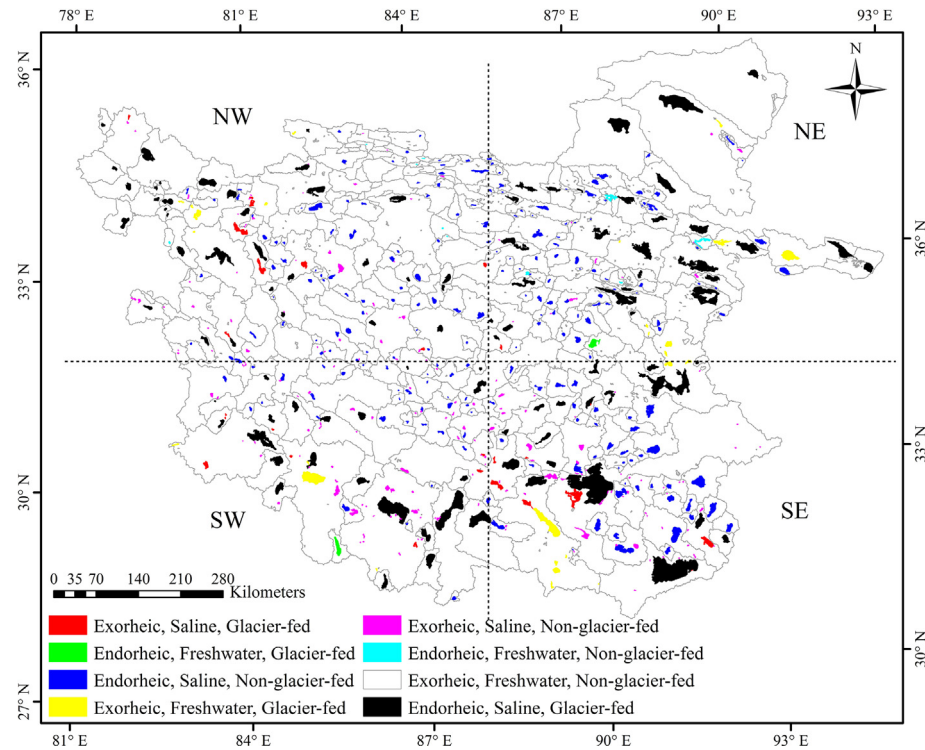


Fig. 6. Spatial distribution of different lake types.

CP lake expansion is still under debate. Some researchers argued that the expansion was largely due to glacier melting (Duo et al., 2010; Yao et al., 2007; Zhang et al., 2011b; Zhu et al., 2010) while others suggested that increasing precipitation may exert a greater impact (Lei et al., 2013; Song et al., 2014b; Zhou et al., 2015). In addition, permafrost thawing caused by temperature increase has been proposed as another paramount driver for lake expansion (Li et al., 2014; Liu et al., 2010). In the following section, the primary potential causes of the lake expansion are discussed. Firstly, we assessed the accuracy of satellite-based climate data and then estimated the relationship between lake area changes and climate factors on the basin scale.

5.1. Accuracy and uncertainty of TRMM precipitation and MODIS LST products

In situ precipitation and temperature observed at the six meteorological stations (51886, 55248, 55294, 55279, 55472, 56223) (see Fig. 1) on the CP were used to validate MODIS LST and TRMM precipitation products. The annual mean of the observed daily minimum temperatures was chosen to validate the night time MODIS LST product. As shown in Fig. 8a and b, MODIS LST agrees well with station-observed temperature ($R^2 = 0.90$, $p < 0.01$), which is consistent with the validation for the entire TP in Zhang et al. (2014a). TRMM precipitation agrees fairly well with station observations ($R^2 = 0.72$, $p < 0.01$), which is also in line with the validation for the entire TP in Li et al. (2014). Due to the lower accuracy of MODIS day-time temperature on the TP (Schneider et al., 2009; Zhang et al., 2014a), only its night time LST was used in this study, which may lead to certain bias in the trend of average temperature (Li et al., 2015). However, the trends of minimum temperature and average temperature at the six meteorological stations have the same changing directions (see Fig. 8), indicating that the bias is very likely to be insignificant.

5.2. Relationship between lake changes and climate factors

Using our yearly mapping of all CP lakes from 2009 to 2014, we explored the relationship between lake dynamics and primary climate factors including precipitation and temperature in each endorheic basin. As shown in Fig. 9, lake expansion occurred in the majority of basins (76%), while lake shrinkage is only found in a few basins distributed mainly in the southwestern region. Lake area changes seem to be more directly associated with precipitation than temperature (Fig. 9). We further summarize the relationship between changes in lake area and climate factors in Fig. 10.

Among the 356 basins with lake existence (Fig. 10a), 196 (55%) basins show positive correlations between lake area and precipitation, and 140 (39%) basins show positive correlations between lake area and temperature. Among the latter, 139 (39%) basins contain permafrost while only 40 (11%) basins contain glacier. This further suggests that glacier melting alone cannot fully explain the observed lake expansion. Among the 271 basins with expanding lake area (Fig. 10b), 169 (62%) basins experienced increasing precipitation, and 70 (26%) basins concurred with rising temperature, in which all 70 (26%) basins contain glacier or permafrost, suggesting that lake expansion seems to be more related to increasing precipitation compared with rising temperature. However, in the northeastern CP, lakes in some basins show rapid expansions (refer back to Fig. 4) but with decreasing precipitation. This regional discrepancy may be attributed to the inherent uncertainty of TRMM precipitation data (see detailed comparison of different precipitation datasets in Fig. S1) (Adler et al., 2003; Xie and Arkin, 1997). In addition, inter- and intra-annual variations in the area of studied large lakes also show closer covariation with precipitation than with temperature in each sub-region (see Fig. S2–S6), which further implies that lake expansion is more related to increasing precipitation.

Although this study provides a high-temporal monitoring of alpine lakes and reveals that the recent lake dynamics may be

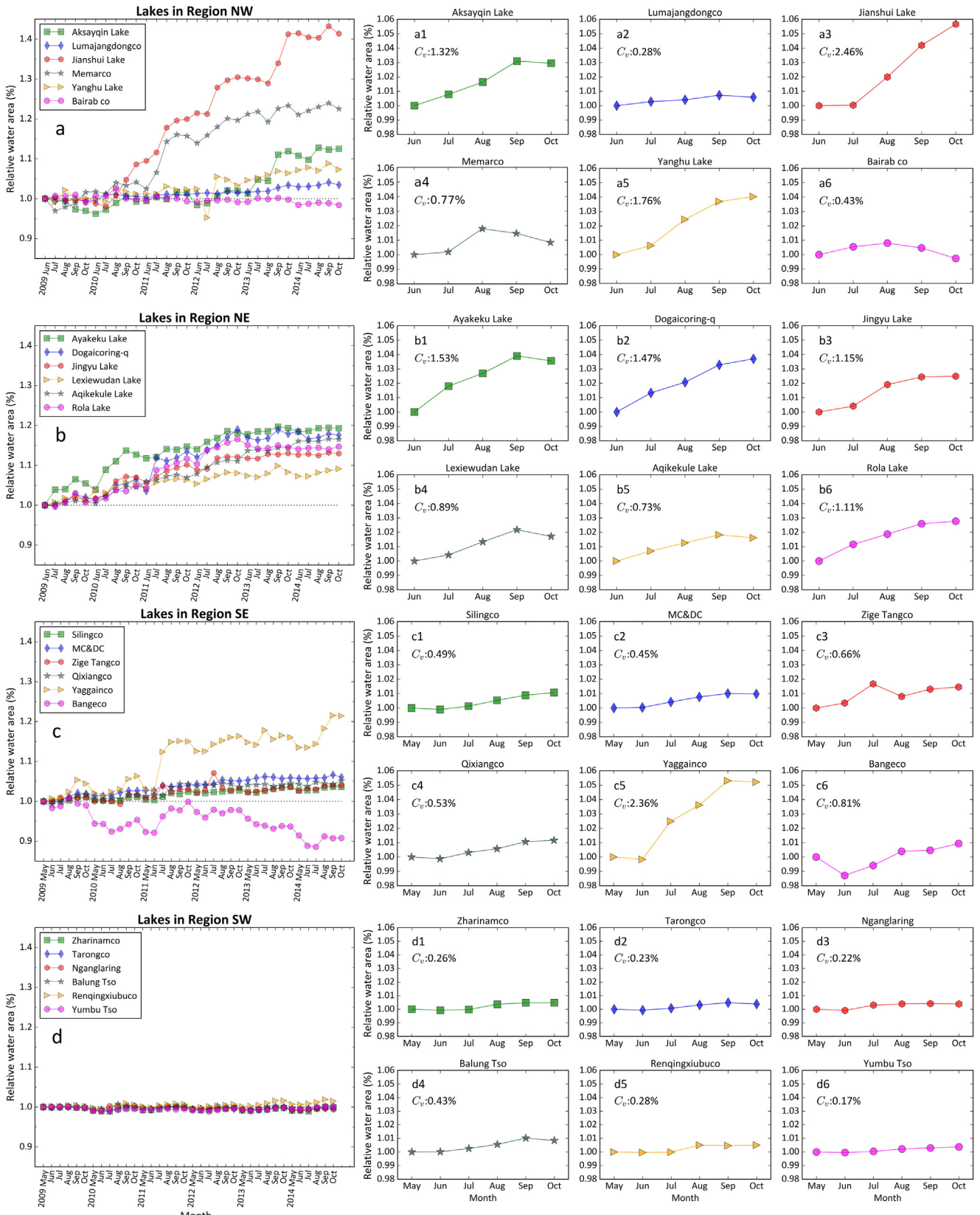


Fig. 7. Inter-annual and intra-annual variations of 24 large lakes in the unfrozen period during 2009–2014. Left (a–d), monthly series of lake areas in region NW, NE, SE and SW, respectively. Right (a1–a6), (b1–b6), (c1–c6), and (d1–d6), average areas in each unfrozen month during 2009–2014 for individual lakes in region NW, NE, SW, and SE, respectively.

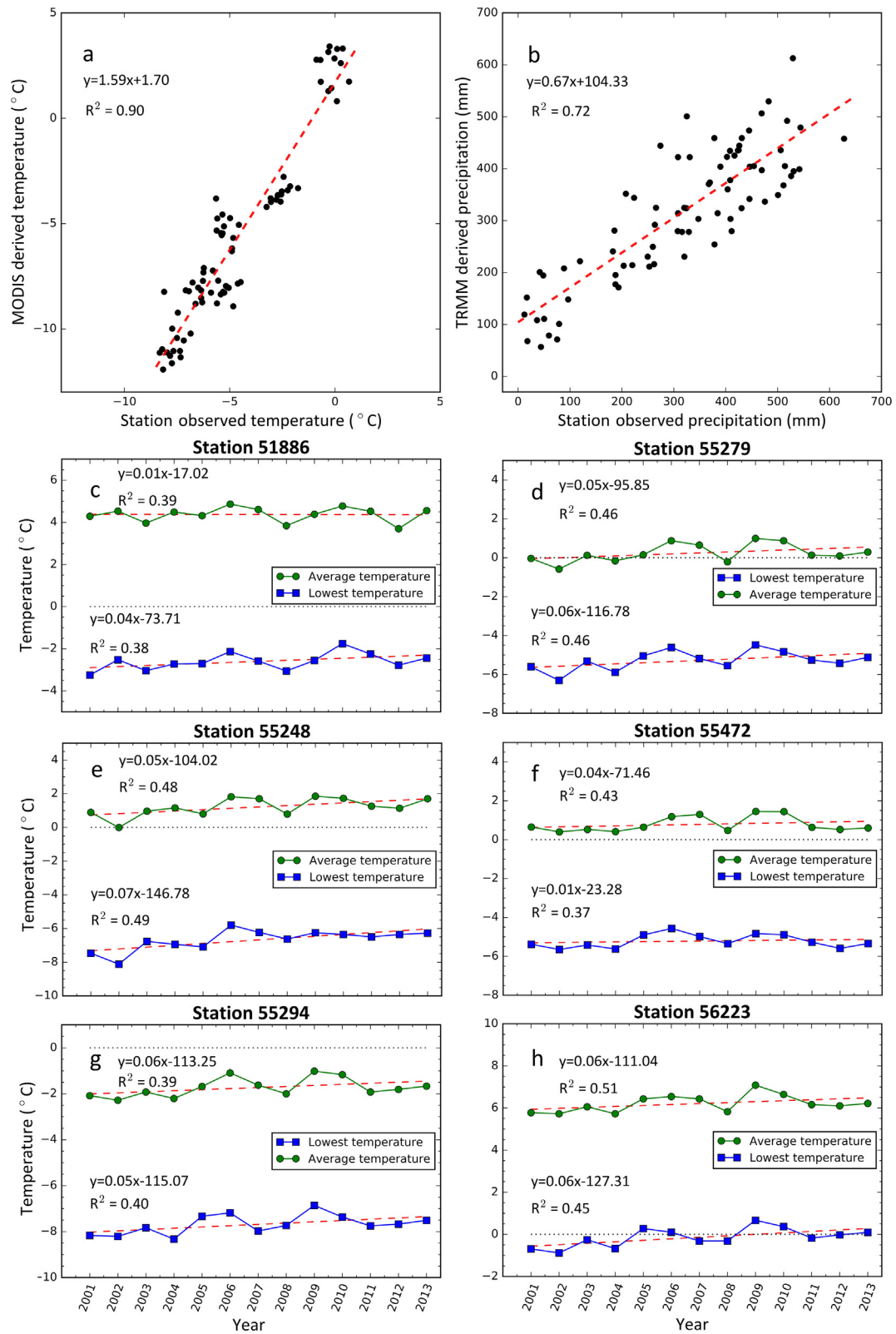


Fig. 8. Validation of MODIS derived temperature and TRMM derived precipitation on the CP during 2001–2013. (a), comparison of MODIS derived temperature with station observed temperature; (b), comparison of TRMM derived precipitation with station observed precipitation; (c)–(h), comparisons between the annual means of daily mean temperature and the annual means of daily minimum temperature at the six meteorological stations (51886, 55248, 55294, 55279, 55472, 56223).

mainly driven by precipitation, we would like to identify a few limitations for possible future improvements. First, our study period is limited to six near-recent years, i.e., 2009–2014. Continuous mon-

itoring is needed to track and better comprehend Tibetan lake changes in the early decades of the new Millennium. Second, our investigation of intra-annual area patterns are focused on 24 lakes

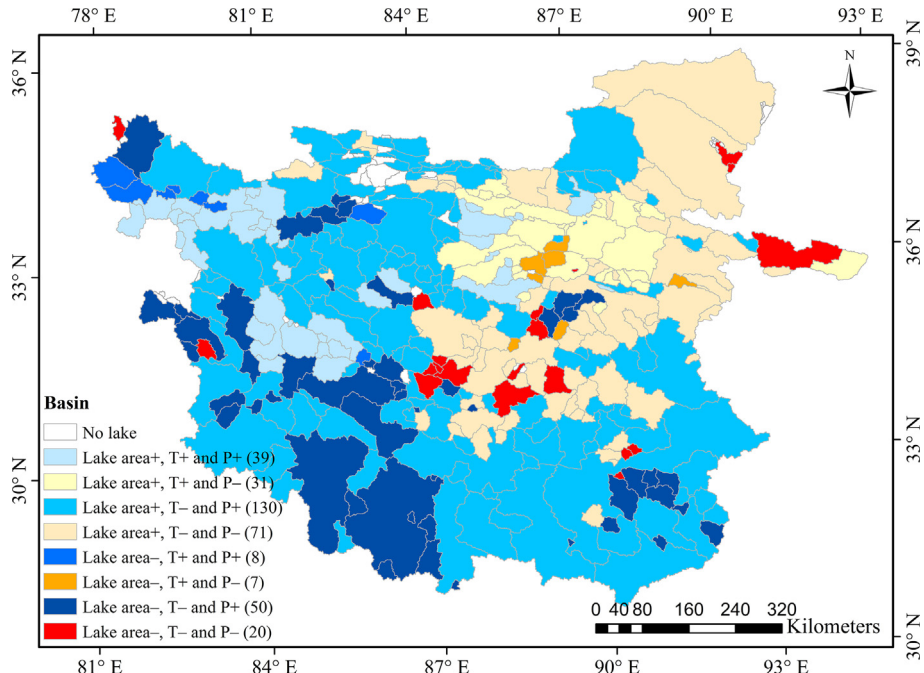


Fig. 9. Trends of lake area, precipitation, and temperature in each endorheic basin on the CP during 2009–2014. 'T' and 'P' stand for temperature and precipitation, respectively, and '+' and '-' increasing and decreasing trends, respectively. Numbers in parentheses indicate the numbers of endorheic basins under different area, precipitation and temperature scenarios.

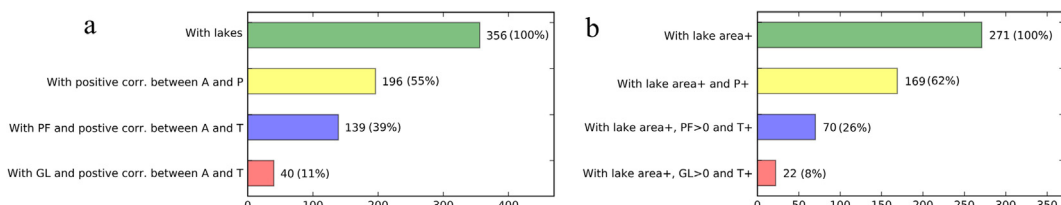


Fig. 10. Correlations between lake area and environmental factors at the basin scale during 2009–2014. (a), basin numbers with lake existence under different environmental conditions; (b) basin numbers with increased lake area under different environmental conditions. A, P and T stand for lake area, precipitation and temperature, respectively, PF and GL existence of permafrost and glacier, respectively, 'area +' increasing lake area, and 'T+' and 'P+' increase of temperature and precipitation, respectively.

larger than 50 km^2). Future inclusions of smaller lakes will provide a more complete understanding of seasonal dynamics of the Tibetan lake system and its responses to climatic and hydrologic changes.

6. Summary and concluding remarks

In this study, we implemented a systematic mapping framework to reveal the inter- and intra-annual variations of alpine lakes on the CP at a 30-m resolution using Landsat and China's HJ satellites data. Lake areas mapped from both satellite sources are highly consistent. Using these multi-mission satellite data, we provided an annual mapping of all alpine lakes bigger than 1 km^2 on the CP and a monthly mapping of 24 large lakes bigger than 50 km^2 with different characteristics for the recent six years (from 2009 to 2014). Our study contributes to alpine lake studies by providing some of finest spatiotemporal details of recent lake dynamics on the critical CP.

During our study period, the total alpine lake area on the CP exhibited an inter-annual increasing trend of $340.79 \text{ km}^2 \text{ yr}^{-1}$ ($1.06\% \text{ yr}^{-1}$, $p < 0.05$). About 98% of the net area increase is attributed to the rapid expansion of endorheic lakes ($334.61 \text{ km}^2 \text{ yr}^{-1}$ or $1.24\% \text{ yr}^{-1}$, $p < 0.05$), while the remaining marginal increase is

explained by exorheic lakes ($6.18 \text{ km}^2 \text{ yr}^{-1}$ or $0.12\% \text{ yr}^{-1}$). Saline lakes, as they are mostly endorheic, experienced a rapid expansion of $326.80 \text{ km}^2 \text{ yr}^{-1}$ ($1.13\% \text{ yr}^{-1}$, $p < 0.05$), whereas freshwater lakes appeared to be highly stable with a changing rate of $13.99 \text{ km}^2 \text{ yr}^{-1}$ ($0.43\% \text{ yr}^{-1}$). Both glacier-fed lakes and non-glacier-fed lakes show substantial expansions by $224.94 \text{ km}^2 \text{ yr}^{-1}$ ($0.92\% \text{ yr}^{-1}$, $p < 0.05$) and $115.85 \text{ km}^2 \text{ yr}^{-1}$ ($1.47\% \text{ yr}^{-1}$, $p < 0.05$), respectively. Although lake area intra-annual variations differ among individual lakes (with coefficient of variation ranging from $\sim 0.2\%$ to $\sim 2.5\%$), most of the studied large lakes had expanded during the unfrozen period and reached to their maximum extents in September or October. Both inter- and intra-annual variations of lake extent revealed a strong spatial heterogeneity. In general, lakes on the northeastern CP experienced rapid expansions, while lakes on the southwestern CP were stable or shrinking.

Our lake change comparisons among different types provide several scientific implications. First, endorheic lakes on the CP are highly sensitive to the variations of water inflow and evaporation, and thus monitoring their changes is of critical importance for understanding regional climate change. Second, expanding saline lakes and stable freshwater lakes, together with glacier retreat and permafrost thawing, suggest that the proportion of freshwater resources on the CP is likely in decline. Third, both glacier-fed and non-glacier-fed lakes experienced rapid expansions, indicating that

glacier retreat alone cannot fully explain the recent lake expansion. Finally, our spatial analysis using climate variables show that increasing precipitation is likely more responsible for the recent lake expansion on the CP, although a more thorough understanding of the lake change mechanism requires future efforts of quantitative attributions to different environmental factors.

Acknowledgements

This study was supported by the Key Program of the National Natural Science Foundation of China (Grant No. 41631179), and the National High Technology Research and Development Program of China (Grant No. 2015AA123901).

Appendix A. Supplementary data

Supplementary data associated with this article can be found, in the online version, at <http://dx.doi.org/10.1016/j.jhydrol.2017.07.024>.

References

- Adler, R.F. et al., 2003. The version-2 Global Precipitation Climatology Project (GPCP) monthly precipitation analysis (1979–Present). *J. Hydrometeorol.* 4 (6), 1147–1167. [http://dx.doi.org/10.1175/1525-7541\(2003\)004<1147:tvgpcp>2.0.co;2](http://dx.doi.org/10.1175/1525-7541(2003)004<1147:tvgpcp>2.0.co;2).
- Arvidson, T., et al., 2002. Validation of the Landsat 7 long-term acquisition plan, *Proceedings of Pecora*. Citeseer.
- Duo, B., Baciren, B., Ba, L., Caiyun, W., Tao, C., 2010. The response of water level of Selin Co to climate change during 1975–2008. *Acta Geographica Sinica* 65 (3), 313–319.
- Ersi, K., Chaohai, L., Zichu, X., Xin, L., Yongping, S., 2010. Assessment of glacier water resources based on the Glacier Inventory of China. *Ann. Glaciol.* 50 (53), 104–110.
- Feyisa, G.L., Meilby, H., Fensholt, R., Proud, S.R., 2014. Automated water extraction index: a new technique for surface water mapping using Landsat imagery. *Remote Sens. Environ.* 140, 23–35. <http://dx.doi.org/10.1016/j.rse.2013.08.029>.
- Guo, W., et al., 2014. The second glacier inventory dataset of China (version 1.0). Cold and Arid Regions Science Data Center: Lanzhou, China.
- Haas, E.M., Bartholomé, E., Lambin, E.F., Vanacker, V., 2011. Remotely sensed surface water extent as an indicator of short-term changes in ecohydrological processes in sub-Saharan Western Africa. *Remote Sens. Environ.* 115 (12), 3436–3445. <http://dx.doi.org/10.1016/j.rse.2011.08.007>.
- Hansen, J., Ruedy, R., Sato, M., Lo, K., 2010. Global surface temperature change. *Rev. Geophys.* 48 (4).
- Huang, L., Liu, J., Shao, Q., Liu, R., 2011. Changing inland lakes responding to climate warming in Northeastern Tibetan Plateau. *Clim. Change* 109 (3–4), 479–502. <http://dx.doi.org/10.1007/s10584-011-0032-x>.
- Huffman, G.J. et al., 2007. The TRMM Multisatellite Precipitation Analysis (TMPA): quasi-global, multiyear, combined-sensor precipitation estimates at fine scales. *J. Hydrometeorol.* 8 (3), 237–247.
- Jiang, H., et al., 2014. An automated method for extracting rivers and lakes from Landsat imagery. *Remote Sens. 6* (6), 5067–5089.
- Jiang, L., Nielsen, K., Andersen, O.B., Bauer-Gottwein, P., 2017. Monitoring recent lake level variations on the Tibetan Plateau using CryoSat-2 SARIn mode data. *J. Hydrol.* 544, 109–124.
- Ju, J., Roy, D.P., 2008. The availability of cloud-free Landsat ETM+data over the conterminous United States and globally. *Remote Sens. Environ.* 112 (3), 1196–1211. <http://dx.doi.org/10.1016/j.rse.2007.08.011>.
- Lehner, B., Verdin, K., Jarvis, A., 2006. HydroSHEDS technical documentation, version 1.0. World Wildlife Fund US, Washington, DC, pp. 1–27.
- Lei, Y. et al., 2014. Response of inland lake dynamics over the Tibetan Plateau to climate change. *Clim. Change* 125 (2), 281–290. <http://dx.doi.org/10.1007/s10584-014-1175-3>.
- Lei, Y. et al., 2013. Coherent lake growth on the central Tibetan Plateau since the 1970s: characterization and attribution. *J. Hydrol.* 483, 61–67.
- Lei, Y. et al., 2012. Glacier mass loss induced the rapid growth of Linggo Co on the central Tibetan Plateau. *J. Glaciol.* 58 (207), 177–184.
- Li, J., Sheng, Y., 2012. An automated scheme for glacial lake dynamics mapping using Landsat imagery and digital elevation models: a case study in the Himalayas. *Int. J. Remote Sens.* 33 (16), 5194–5213.
- Li, J., Sheng, Y., 2013. Spatiotemporal pattern and process of inland lake change in the Qinghai-Tibetan Plateau during the period of 1976–2009. *Arid Zone Res.* 30 (4), 571–581.
- Li, S., Cheng, G., 1996. Map of permafrost distribution on the Qinghai-Xizang (Tibetan) Plateau, scale 1: 3,000,000. Gansu Cultural Press, Lanzhou [in Chinese].
- Li, Y., Liao, J., Guo, H., Liu, Z., Shen, G., 2014. Patterns and potential drivers of dramatic changes in Tibetan lakes, 1972–2010. *PLoS One* 9 (11), e111890. <http://dx.doi.org/10.1371/journal.pone.0111890>.
- Li, Z., Wang, K., Zhou, C., Wang, L., 2015. Modelling the true monthly mean temperature from continuous measurements over global land. *Int. J. Climatol.* 36 (4), 2103–2110.
- Liao, A. et al., 2014. High-resolution remote sensing mapping of global land water. *Sci. Chin. Earth Sci.* 57 (10), 2305–2316.
- Liao, J., Shen, G., Li, Y., 2013. Lake variations in response to climate change in the Tibetan Plateau in the past 40 years. *Int. J. Digital Earth* 6 (6), 534–549. <http://dx.doi.org/10.1080/17538947.2012.656290>.
- Liu, J., Kang, S., Gong, T., Lu, A., 2010. Growth of a high-elevation large inland lake, associated with climate change and permafrost degradation in Tibet. *Hydrol. Earth Syst. Sci.* 14 (3), 481–489.
- Lu, S., Wu, B., Yan, N., Wang, H., 2011. Water body mapping method with HJ-1A/B satellite imagery. *Int. J. Appl. Earth Obs. Geoinf.* 13 (3), 428–434. <http://dx.doi.org/10.1016/j.jag.2010.09.006>.
- Lyons, E.A. et al., 2013. Quantifying sources of error in multitemporal multisensor lake mapping. *Int. J. Remote Sens.* 34 (22), 7887–7905. <http://dx.doi.org/10.1080/01431161.2013.827343>.
- McFeeters, S.K., 1996. The use of the Normalized Difference Water Index (NDWI) in the delineation of open water features. *Int. J. Remote Sens.* 17 (7), 1425–1432.
- Pekel, J.-F., Cottam, A., Gorelick, N., Belward, A.S., 2016. High-resolution mapping of global surface water and its long-term changes. *Nature*.
- Phan, V.H., Lindenbergh, R.C., Menenti, M., 2013. Geometric dependency of Tibetan lakes on glacial runoff. *Hydrol. Earth Syst. Sci. Discuss.* 10 (1), 729–768. <http://dx.doi.org/10.5194/hessd-10-729-2013>.
- Qiao, C. et al., 2012. An adaptive water extraction method from remote sensing image based on NDWI. *J. Indian Soc. Remote Sens.* 40 (3), 421–433.
- Qiu, J., 2008. China: the third pole. *Nature News* 454 (7203), 393–396.
- Rangwala, I., Miller, J.R., Xu, M., 2009. Warming in the Tibetan Plateau: possible influences of the changes in surface water vapor. *Geophys. Res. Lett.* 36 (6).
- Rizvi, J., 1999. Trans-Himalayan Caravans: Merchant Princes and Peasant Traders in Ladakh. Oxford University Press, New Delhi.
- Schneider, P. et al., 2009. Satellite observations indicate rapid warming trend for lakes in California and Nevada. *Geophys. Res. Lett.* 36 (22).
- Sheng, Y. et al., 2016. Representative lake water extent mapping at continental scales using multi-temporal Landsat-8 imagery. *Remote Sens. Environ.* 185, 129–141.
- Sheng, Y., Yao, T., 2009. Integrated assessments of environmental change on the Tibetan Plateau. *Environ. Res. Lett.* 4 (4), 045201. <http://dx.doi.org/10.1088/1748-9326/4/4/045201>.
- Song, C., Huang, B., Ke, L., 2013. Modeling and analysis of lake water storage changes on the Tibetan Plateau using multi-mission satellite data. *Remote Sens. Environ.* 135, 25–35.
- Song, C., Huang, B., Ke, L., 2014a. Inter-annual changes of alpine inland lake water storage on the Tibetan Plateau: detection and analysis by integrating satellite altimetry and optical imagery. *Hydrol. Process.* 28 (4), 2411–2418. <http://dx.doi.org/10.1002/hyp.9798>.
- Song, C., Huang, B., Richards, K., Ke, L., Hien Phan, V., 2014b. Accelerated lake expansion on the Tibetan Plateau in the 2000s: induced by glacial melting or other processes? *Water Resour. Res.* 50 (4), 3170–3186.
- Song, C., Sheng, Y., Ke, L., Nie, Y., Wang, J., 2016. Glacial lake evolution in the southeastern Tibetan Plateau and the cause of rapid expansion of proglacial lakes linked to glacial-hydrogeomorphic processes. *J. Hydrol.* 540, 504–514.
- Song, C. et al., 2017. Heterogeneous glacial lake changes and links of lake expansions to the rapid thinning of adjacent glacier termini in the Himalayas. *Geomorphology* 280, 30–28.
- Wan, W. et al., 2016. A lake data set for the Tibetan Plateau from the 1960s, 2005, and 2014. *Sci. Data* 3, 160039. <http://dx.doi.org/10.1038/sdata.2016.39>.
- Wang, J., et al., 2015. A high-resolution global lake inventory with classified freshwater and saline types. American Geophysical Union: San Francisco, California, December 14–18, 2015.
- Wang, J., Sheng, Y., Tong, T.S.D., 2014. Monitoring decadal lake dynamics across the Yangtze Basin downstream of Three Gorges Dam. *Remote Sens. Environ.* 152, 251–269.
- Wang, J., et al., 2016. Progress of global lake inventory: freshwater and saline lakes. AAG Great Plains/Rocky Mountains Regional Division Fall Meeting: Colorado Springs, Colorado, October 21–22, 2016.
- Wang, S., Dou, H., 1998. *Chinese Lake Catalogue*. Science Press, Beijing.
- Williamson, C.E., Saros, J.E., Vincent, W.F., Smold, J.P., 2009. Lakes and reservoirs as sentinels, integrators, and regulators of climate change. *Limnology and Oceanography*, 54(6part2), pp. 2273–2282.
- Xie, P., Arkin, P.A., 1997. Global precipitation: a 17-year monthly analysis based on gauge observations, satellite estimates, and numerical model outputs. *Bull. Am. Meteorol. Soc.* 78 (11), 2539–2558. [http://dx.doi.org/10.1175/1520-0477\(1997\)078<2539:gpmay>2.0.co;2](http://dx.doi.org/10.1175/1520-0477(1997)078<2539:gpmay>2.0.co;2).
- Xu, Z.X., Gong, T.L., Li, J.Y., 2008. Decadal trend of climate in the Tibetan Plateau—regional temperature and precipitation. *Hydrol. Process.* 22 (16), 3056–3065. <http://dx.doi.org/10.1002/hyp.6892>.
- Yang, M., Nelson, F.E., Shiklomanov, N.I., Guo, D., Wan, G., 2010. Permafrost degradation and its environmental effects on the Tibetan Plateau: a review of recent research. *Earth Sci. Rev.* 103 (1), 31–44.
- Yao, F. et al., 2015. High-resolution mapping of urban surface water using ZY-3 multi-spectral imagery. *Remote Sens.* 7 (9), 12336–12355.

- Yao, T., Pu, J., Lu, A., Wang, Y., Yu, W., 2007. Recent glacial retreat and its impact on hydrological processes on the Tibetan Plateau, China, and surrounding regions. *Arct. Antarct. Alp. Res.* 39 (4), 642–650.
- Yao, T. et al., 2012. Different glacier status with atmospheric circulations in Tibetan Plateau and surroundings. *Nat. Clim. Change* 2 (9), 663–667.
- Zhang, B. et al., 2011a. Estimation and trend detection of water storage at Nam Co Lake, central Tibetan Plateau. *J. Hydrol.* 405 (1), 161–170.
- Zhang, G., Xie, H., Duan, S., Tian, M., Yi, D., 2011b. Water level variation of Lake Qinghai from satellite and in situ measurements under climate change. *J. Appl. Remote Sens.* 5 (1), 053532-053532-15.
- Zhang, G. et al., 2014a. Estimating surface temperature changes of lakes in the Tibetan Plateau using MODIS LST data. *J. Geophys. Res.: Atmos.* 119 (14), 8552–8567.
- Zhang, G., Yao, T., Xie, H., Zhang, K., Zhu, F., 2014b. Lakes' state and abundance across the Tibetan Plateau. *Chin. Sci. Bull.* 59 (24), 3010–3021. <http://dx.doi.org/10.1007/s11434-014-0258-x>.
- Zhang, G. et al., 2017a. Extensive and drastically different alpine lake changes on Asia's high plateaus during the past four decades. *Geophys. Res. Lett.*
- Zhang, G. et al., 2017b. Lake volume and groundwater storage variations in Tibetan Plateau's endorheic basin. *Geophys. Res. Lett.*
- Zhou, J. et al., 2015. Exploring the water storage changes in the largest lake (Selin Co) over the Tibetan Plateau during 2003–2012 from a basin-wide hydrological modeling. *Water Resour. Res.* 51 (10), 8060–8086.
- Zhu, L., Xie, M., Wu, Y., 2010. Quantitative analysis of lake area variations and the influence factors from 1971 to 2004 in the Nam Co basin of the Tibetan Plateau. *Chin. Sci. Bull.* 55 (13), 1294–1303.